Journal of Drug Delivery Science and Technology 108 (2025) 106873

Contents lists available at ScienceDirect

Journal of Drug Delivery Science and Technology

journal homepage: www.elsevier.com/locate/jddst

3D printed mucoadhesive bupropion hydrochloride buccal thin films using Liquid Crystal Display

Chrystalla Protopapa [a], Angeliki Siamidi [a], Laura Andrade Junqueira [d], Siva Kolibaka [b], Hossam Ahmed [c], Joshua Boateng [c], Dennis Douroumis [b,*], Marilena Vlachou [a,**]

[a] Section of Pharmaceutical Technology, Department of Pharmacy, National and Kapodistrian University of Athens, 157 84, Athens, Greece
[b] Centre for Research Innovation, University of Greenwich, Medway Campus, Chatham Maritime, Chatham, ME4 4TB, UK
[c] School of Science, University of Greenwich, Medway Campus, Chatham Maritime, Chatham, ME4 4TB, UK
[d] Delta Pharmaceutics Ltd., 1-3 Manor Street, ME4 6AE, Chatham, UK

ARTICLE INFO

Keywords:
3D printing
Liquid crystal display (LCD)
Buccal films
Personalized medicine
Bupropion hydrochloride

ABSTRACT

Oromucosal delivery of active pharmaceutical ingredients offers a promising alternative method of administration, as it bypasses the first-pass metabolism and enhances patient compliance especially for people who have difficulties swallowing. In this study, liquid crystal display (LCD) 3D printing was explored as an additive manufacturing process for producing mucoadhesive thin films of various sizes containing bupropion hydrochloride (BUP·HCl). For this purpose, poly(ethylene) oxide (polyox 10N) was used as a mucoadhesion enhancer, while PEG200 was used as a plasticizer to form flexible BUP·HCl buccal films, and PEGDA700 served as a crosslinking agent. Solid-state analysis was carried out using differential scanning calorimetry (DSC and X-ray diffraction) which showed that BUP·HCl was in amorphous state within the printed films.

The swelling ratio of the thin films varied from 0.9 to 1.3 while ink composition resulted peak adhesive force values of 0.37–0.52Nmm and cohesiveness values between 8 and 9 mm affected by the content of poly(ethylene) oxide. Dissolution studies in simulated saliva showed immediate release for all the BUP·HCl thin films while the *ex vivo* permeability in porcine buccal epithelium revealed 52 % permeation within 120 min. The results demonstrated that LCD printing technology is a robust, time-efficient, and high precision technology that can be used for the design of personalized medications.

1. Introduction

As each patient has different metabolism, age, weight and height, the current 'one size fits all' treatment approach is inefficient [1–5]. It is noteworthy that when this approach is used, only 30–60 % of patients receive effective treatment, whereas personalizing treatment for each individual based on their needs can lead to improved outcomes [6–8].

One of the most widespread approaches for the design and development of personalized medicines is the utilization of 3D printers [9–11]. In the realm of 3D printing, an additive manufacturing technique, the process begins with crafting the initial design of the desired part [12,13]. This design is created using computer software compatible with 3D printers, which then generates a specific file format to send to the printer [14–16]. The printer interprets this file, constructing the product layer by layer. Almost all 3D printing processes rely on layering to shape a part. Consequently, 3D printers perceive each part as a series of individual two-dimensional layers rather than as a unified whole [17].

A few studies have been reported where 3D printing technologies were introduced for the development of novel buccal films. Eleftheriadis et al. employed Fused Deposition Modelling (FDM) for the preparation of diclofenac mucoadhesive buccal films [18]. Additionally, Abdella et al. and Chachlioutaki et al., used microextrusion, to develop 3D printed bilayer mucoadhesive buccal film of estradiol and oromucosal pullulan films of chlorpromazine hydrochloride respectively [19,20]. Elbadawi et al. utilized dual-nozzle pressure-assisted microsyringe for the preparation of oral films based on pullulan and hydroxypropyl methylcellulose [21].Furthermore, Jovanovic et al. created prolonged release of Propranolol Hydrochloride with the use of semi-solid extrusion [22]. However, none of the available research has used any VAT

* Corresponding author.
** Corresponding author.
E-mail address: d.douroumis@gre.ac.uk (D. Douroumis).

https://doi.org/10.1016/j.jddst.2025.106873
Received 29 October 2024; Received in revised form 1 February 2025; Accepted 29 March 2025
Available online 4 April 2025
1773-2247/© 2025 The Authors. Published by Elsevier B.V. This is an open access article under the CC BY license (http://creativecommons.org/licenses/by/4.0/).

photopolymerization 3D printer, particularly the newer liquid crystal display (LCD) type, for the preparation of buccal films.

Bupropion (BUP) is an antidepressant with unique mechanisms, used for a variety of conditions beyond depression. These include smoking cessation, depression, weight loss, ADHD management, seasonal affective disorder, and possibly amphetamine dependence [23–26]. Unlike many antidepressants, BUP does not cause drowsiness and is more effective than SSRIs in improving hypersomnia and fatigue in depression [27–31]. It is available as immediate and sustained release formulations [27,32,33]. Therapeutic doses for patients can differ significantly, ranging from 75 mg to 522 mg for once-daily administration [34]. However, commercially available tablets are produced in a limited number of fixed strengths for 12-h and 24-h formulations [34]. As a result, patients often need to combine different doses or alternate dosages on different days. This increases the risk of confusion, medication errors, and non-adherence, potentially leading to severe side effects or reduced treatment effectiveness. BUP when administered intravenously, is immediately absorbed and achieves 100 % bioavailability. This is in contrast to the oral route, where absorption is delayed, undergoes first-pass metabolism, and its absolute bioavailability remains undetermined, potentially ranging as low as 5–20 % [35,36]. Although increasingly embraced by the medical field, BUP presents a notable obstacle: its narrow therapeutic range. This feature puts patients at risk for delayed symptom onset with extended-release forms and potentially severe consequences in cases of overdose [35]. Notably, documented evidence highlights the heightened risk of seizures, even within recommended dosage ranges, due to its narrow therapeutic window [37]. Additionally, its effect on cardiac conduction is firmly established and proves resistant to conventional treatment methods [38].

In recent years, there has been a rising awareness among researchers of the crucial role patients play in the drug development journey, leading to the concept of 'patient-centricity' [39]. Within the realm of pharmaceutics, this idea can be strengthened through the modification of drug formulations, providing an attractive strategy for drug developers. For example, converting orally administered tablets into buccal drug delivery systems provides a promising solution for patients experiencing swallowing difficulties or when it's necessary to bypass the first-pass metabolism. This approach helps avoid absorption through the gastrointestinal tract, directing the medication straight to systemic circulation [40].

Buccal drug delivery involves administering medications to the buccal mucosa, found on the inner cheek inside the mouth, and can aid in delivering drugs locally or systemically [41]. This method circumvents initial metabolism, enzymatic degradation of drugs, and offers effective treatment for patients who cannot swallow or have difficulty swallowing [42]. Patients tend to prefer mucoadhesive buccal films over buccal tablets, as they offer greater flexibility for increased comfort and can be tailored to individual sizes [41,47]. Such films consist of several layers and are mainly used for prolonged drug release in the mouth [43]. Buccal films today are used extensively in many therapeutic cases like cardiovascular disease, antiemetic, anti-inflammatory, anaesthetic etc. [44,45,47].

In the present study, we report for first time the development of BUP·HCl buccal thin films by using LCD technology. The technology offers rapid printing with high accuracy and reproducibility while the film dimensions can be easily adjusted and hence to develop personalized medicines with the desired dose strength.

2. Materials and methods

The active ingredient BUP in the form of its hydrochloride salt (BUP·HCl) (MW: 276.20), the excipient PEG200 (MW:200), and the photoinitiator phenyl-bis(2,4,6-trimethylbenzoyl)phosphine oxide (TPO) (MW: 418.47) were purchased from the Tokyo Chemical Ltd. (Tokyo, Japan). The polyox 10N (MW: 100,000) was obtained from Colorcon (Dartford, UK). The excipient PEGDA700 (MW: 700) was purchased from Sigma–Aldrich Ltd. (Steinheim, Germany). All the aforementioned excipients are of pharmaceutical grade.

2.1. Three-dimensional printing

PEGDA served as the photopolymerisable monomer, while TPO was used as the photoinitiator (PI). Table 1 shows the formulation that was used for the films' preparation.

All the ingredients were weighed using an ATX224® high-precision analytical balance (Shimadzu, Kyoto, Japan). For the ink preparation BUP·HCl was dissolved in water at room temperature under continuous stirring with the use of magnetic stirrer (PCE-MSR 450, Manchester, UK). Polyox 10N was then added and the mixture was sonicated with the use of LBS 2 Ultrasonic bath (4.5 lt, 285W, 59 KHz), (FALC INSTRUMENTS, Treviglio, Italy), for approximately 20 min or until a sticky solution was formed. PEG200 and PEGDA700, were cautiously added and the resulting mixture was stirred for an additional 10 min to ensure uniformity. Subsequently, TPO was added to the stirred formulation and the mixture was stirred for an additional 4 h. To prevent polymerization and premature solidification, a protective cover was used to shield the mixture from UV radiation. The mixture was then poured onto resin trays, for the subsequent printing processes.

As shown in Fig. 1, four different dimensions of buccal films, 15x17 × 0.1 mm, 16x30 × 0.1 mm, 18x32 × 0.1 mm and 24x35 × 0.1 mm length, width and height, respectively; were designed in AutoCAD® 2023 (Autodesk Inc, San Rafael, CA, USA), exported as a stereolithographic file (.stl) and printed using an LCD 3D printer (Creality, Shenzhen, China). The printer was equipped with a 405 nm laser, enabling the creation of objects with precise resolution accuracy of 0.034 mm, and the production of layers with thickness ranging from 0.005 to 0.2 mm at a printing speed of 1–4 s per layer. The buccal films were printed directly onto the build platform, at ambient temperature, without support. After printing, the films were carefully removed and cleaned with deionized water. Any excess of uncured liquid formulation was removed by blotting with filter paper. Then the films were cured for an additional 2 min under UV light to ensure full polymerization.

2.2. Buccal films physical characteristics

The weight of the buccal films and their dimensions (length, width and height) were assessed using a 4-digit scale and a Vernier caliper, respectively. Each measurement was conducted ten times to ensure accuracy.

2.3. X-ray powder diffraction (XRPD)

X-ray powder diffraction patterns of bulk BUP·HCl, placebo buccal films, buccal films containing BUP·HCl and of the excipient polyox 10N were obtained using a D8 Advance diffractometer (Bruker, Karlsruhe, Germany) with Cu Kα radiation (40 kV, 40 mA) in transmission mode and a LynxEye silicon strip detector. Data were collected with a step size of 0.02° and a counting time of 0.3 s per step, covering the angular range from 5 to 60° 2θ.

Table 1
Shows the composition of the developed formulation.

Materials	Formulation (%w/w)
BUP·HCl	5
PEGDA700	26
PEG200	30
polyox 10N	3
H_2O	35
photoinitiator	1

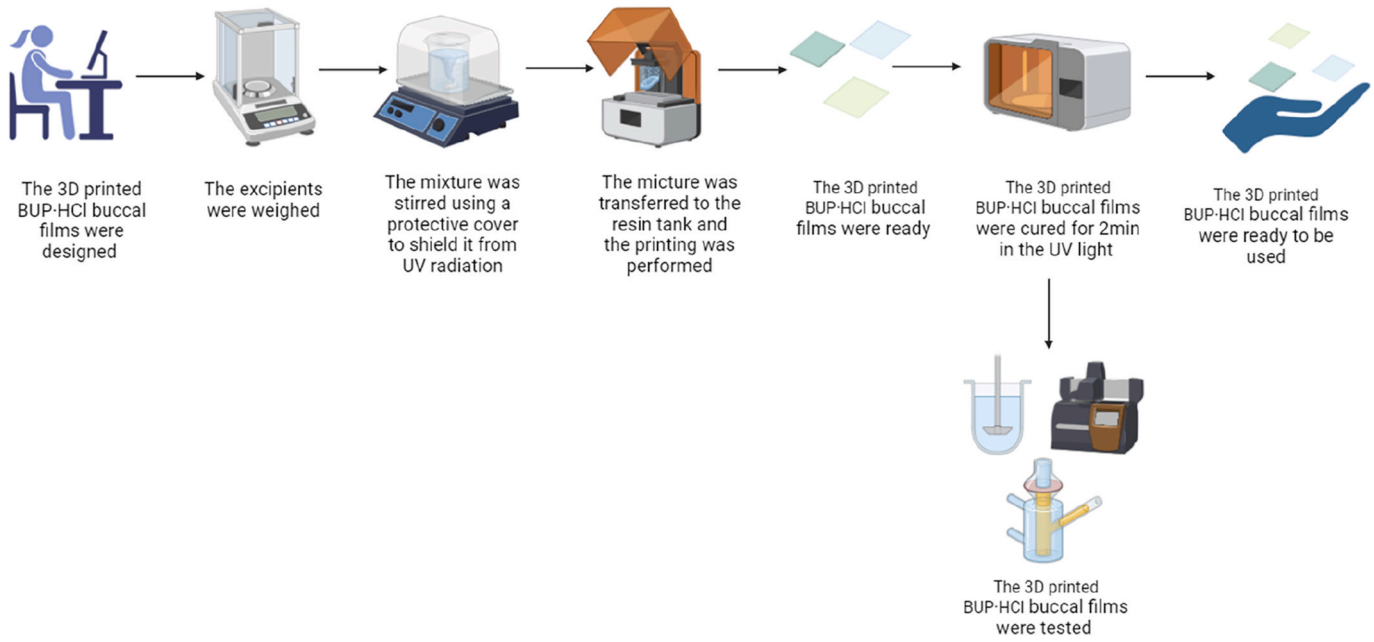

Fig. 1. The methodology of producing 3D BUP·HCl buccal films; created using BioRender.com https://www.biorender.com/(accessed on June 20, 2024).

2.4. Differential scanning calorimetry (DSC)

Thermal analysis of the BUP·HCl drug, placebo film, and film, containing BUP·HCl, was conducted using a DSC-3 (Mettler Toledo, Switzerland), which measures the energy absorbed or released by a sample during heating or cooling. Each sample (4 mg) was precisely weighed using an aluminum pan and hermetically sealed with a lid. The pure BUP·HCl and buccal film formulations were tested. The thermograms were recorded over a temperature range of 25 °C–250 °C, with a heating rate of 10 °C per minute and a continuous nitrogen gas flow of 20 mL per minute. An empty aluminum pan served as the reference.

2.5. Thermal Gravimetric Analysis (TGA)

Thermal gravimetric analysis (TGA) of BUP·HCl was carried out using a TGA Q5000 apparatus (Thermal Instruments, Moraine, OH, USA) to assess its thermal stability. An aluminum pan weighing 54.42 mg was loaded with 6.9 mg of the drug, bringing the total weight to 61.32 mg. The analysis was performed across a temperature range of 25 °C–350 °C, with a heating rate of 10 °C per minute.

2.6. SEM analysis

Electron microscopy (Hitachi SU8030, Japan) was used to evaluate the surface and morphology of the buccal films. SEM images of the 3D-printed buccal film compartments were obtained using an electron beam with an accelerating voltage of 1 kV and magnifications of 100X, 110X, and 250X of the surface, the side view and a closer view of the side view respectively.

2.7. Determination of drug concentration

To measure drug concentration, the buccal films were first milled into powder using a mortar and pestle. The powder was then dissolved in deionized water (1 L) and magnetically stirred continuously with a magnetic stirrer for 24 h. The solution was subsequently filtered using 0.45 μm pore size filters from Millipore Ltd. (Dublin, Ireland). The drug concentration in the solution was determined using a UV–VIS spectrophotometer (uniSPEC 2 Spectrophotometer, LLG Labware, Meckenheim, Germany) at a wavelength of 251 nm. This procedure was repeated three times to ensure measurement accuracy.

2.8. Dissolution studies

The BUP·HCl release from the four different film sizes was measured using a USP II dissolution paddle apparatus (PharmaTest-D17, Hainburg, Germany), at 50 rpm and 37 ± 0.5 °C in an aqueous medium of 500 ml (pH = 6.8) based on previous publications [46–49]. The pH was maintained at 6.8 to replicate the conditions of the oral mucosa and it was measured with Multi 3410 Set 1 pH meter (Wissenschaftlich-TechnischeWerkstätten GmbH, Weilheim, Germany) [47]. Samples of 5 mL were collected every 30 s. Each sample was filtered through 0.45 μm pore size filters (Millipore Ltd., Ireland) and analyzed with a UV–VIS spectrophotometer (uniSPEC 2 Spectrophotometer, LLG Labware, Meckenheim, Germany) at λ_{max} = 251 nm. The dissolution tests were performed three times, resulting in a graph that depicts the percentage release (mean ± standard deviation) over time.

2.9. Ex vivo permeation studies

The ability of BUP·HCl from the buccal film to permeate through the buccal mucosa was assessed using porcine buccal mucosa and Franz diffusion cells (PermeGear, Inc., PA, USA). The porcine buccal mucosa was collected from a local slaughterhouse (Forge Farm Ltd, Kent, UK) immediately after animal processing. The tissue was placed in a refrigerated container (4 °C) for transportation to the laboratory. Upon arrival, the non-keratinized epithelium was carefully separated from the underlying muscle and connective tissue using scissors and scalpel blades, ensuring a uniform thickness of approximately 500 μm. The biological material was stored at −20 °C until the experiments were conducted.

Before the permeation study, the buccal mucosa was defrosted and cut into circular sections suitable for Franz cells. The buccal mucosa samples were mounted on the donor compartments of a Franz diffusion cell and the temperature of the system was maintained at 37 °C using an automated water bath (Thermo Fisher Scientific, Newington, USA). During the experiment, the flow of phosphate buffer (pH 6.8) was constant at a rate of 6.6 mL/h. Initially, the system was equilibrated for 1 h, and a blank sample was collected during this period. Following equilibration, the buccal films were placed above the porcine buccal

mucosa, and the samples were collected at predetermined time points (12, 42, 72, 102, 122 min) using an auto-sampler (FC 204 fraction collector, Gilson, USA). The quantification of BUP·HCl in the samples was performed with a UV–VIS spectrophotometer as previously described. In addition, the blank was also evaluated using UV–Vis, ensuring no interferences were present at the specific wavelength used for quantification. A total diffusion area of 1.77 cm^2 was used to assess the BUP·HCl release into the porcine buccal mucosa. As the films were cut to fit the Franz cell, only the formulation was evaluated, not the size of the films. The results were expressed as the percentage of BUP permeated over time. Additionally, the steady-state flux (J_S) was determined as the slope of the linear portion of the plot of cumulative drug permeated ($\mu g/cm^2$) versus time (h), and the lag time (T_L) represented the x-intercept.

2.10. Water loss rate

Water evaporation through the film was monitored by periodic weighing. The buccal films were printed, cross-linked, and placed in Petri dishes at ambient temperature for 10 h. The films were weighed every 25 min during the first 4 h, and again after 10 h, to monitor weight loss over time. The weight loss indicated the evaporation of water molecules. The relative water weight of the film (calculated as the water weight at each time point divided by the initial water weight) can be determined using Equation (1).

$$W\ (\%) = \frac{Wwt}{Wwo} x100 \quad (1)$$

where W_{wt} is the water weight in the film at every t and W_{w0} the initial weight of water in the film.

2.11. Determination of swelling ratio (SR)

Buccal films of the four different dimensions (15x17 × 0.1 mm, 16x30 × 0.1 mm, 18x32 × 0.1 mm, 24x35 × 0.1 mm) were weighed dry (Md) and then immersed in a pH 6.8 aqueous medium for 24 h at 37 ± 0.5 °C to simulate dissolution test conditions. During the first 2 h, the films were weighed every 10 min, and for the remaining 6 h, they were weighed hourly. In each instance, excess water was carefully removed before weighing (Ms). The swelling ratio (SR) was calculated using the following equation:

$$SR = \frac{Ms - Md}{Md} \quad (2)$$

where *Ms* and *Md* represent the masses of the swollen and dried samples, respectively.

2.12. Texture analyses (adhesion and puncture tests)

The in-vitro adhesion properties of the film were evaluated using a TA HD Texture Analyzer (Stable Microsystem Ltd., Surrey, UK) equipped with a Texture Exponent 32 software. A cylindrical stainless-steel probe (35 mm diameter, p/35) was affixed to each film sample using double-sided adhesive tape. To simulate the buccal environment, a gelatin gel (6.67 % w/w) was prepared and allowed to set, after which 500 μL of simulated saliva at pH 6.8 was spread over the gelatin surface. The film sample attached to the probe, was gradually lowered until contact was established with the gelatin gel surface and contact maintained for 60 s using an applied force of 1 N and the probe withdrawn at the specified speed. The following settings were applied during the test: pre-test and test speeds: 0.5 mm/s; post-test speed: 1 mm/s; trigger force: 0.05 N and return distance: 10 mm. Three key adhesive parameters were measured (i) Peak Adhesive Force (PAF) which is the maximum force required to separate the film sample from the gelatin gel surface; (ii) Work of Adhesion (WOA) calculated as the area under the force-distance curve, representing the total work required for detachment and (iii) Cohesiveness measured as the total distance (mm) travelled by the dressing until complete separation from the gel surface. For the puncture strength, the films were gently taped between the two metal grips of the lower tensile probe (grip) allowing enough space below the films for probe to puncture. The 2 mm cylindrical probe was attached and programmed to penetrate each formulation (test mode: compression; target mode: distance) until it completely punctured the film. The following settings were applied: pre-test speed (1.0 mm/s), test-speed (0.2 mm/s); post-test speed (10.0 mm/s, distance of 5 mm; and trigger force of 0.9g. The maximum force in grams required to completely puncture each film was measured as the puncture strength for each formulation. All measurements were performed in triplicate (n = 3) for each formulation to ensure reproducibility.

3. Results and discussion

3.1. Printing process

In this study, LCD 3D printing was successfully utilized to produce BUP·HCl buccal films. A major advantage of the LCD printer is its easiness of use, which does not require specialized skills from the operator to prepare and print the films. However, a significant limitation is the photosensitivity of the mixture, which must be carefully protected from UV light to avoid early solidification. The objective of this work was to create personalized buccal thin films of BUP·HCl. Fig. 2, illustrates the fabrication of 3D printed thin films of various sizes.

There are several studies where VAT photopolymerization techniques such as LCD, DLP, and SLA have been used to print personalized tablets containing up to six different drugs, with various shapes, modified release profiles, and Braille patterns for visually impaired patients [50–55]. These printed tablets provide a convenient and economical solution, as they can be quickly produced in a single step, while they are easily identified by the patients. However, to the best of our knowledge and up to date, there is not any other study that prints any buccal films using an LCD printer. Almeida et al. developed bilayer buccal films containing BUP using ultrapure sodium carboxymethylcellulose, hydroxypropylmethylcellulose K4M, and medium-viscosity chitosan. The cytotoxicity tests that they performed revealed that the films containing BUP did not cause any cellular damage [56].

The formulation composition and the printing parameters were optimized using a trial-and-error approach to ensure that the printed films presented consistent shape and thickness. For example, a layer thickness of 0.010 mm was selected from a range of 0.005 mm–0.200 mm, as it was shown that at this thickness, the layers of the films solidified well and were shaped uniformly. The same applies to the exposure time and the initial exposure time. These were set to 4.5 s and 60 s, respectively, within ranges of 1–10 s and 10–70 s, as it was shown that these durations resulted in optimal solidification. The adjusted parameters controlling the printing process are outlined in Table 2.

As shown in Fig. 2, the production time of well-defined thin films, was only 2.3 min. The efficiency of the process was further demonstrated by the ability to print simultaneously in 2.3 min approximately 45 buccal films of 15x17 × 0.1 mm and 24 buccal films of 16x30 × 0.1 mm (Fig. 2C) on the building platform. The rapid printing times hold great potential, as healthcare professionals can easily produce personalized medicines for different patient populations within a short timeframe.

Overall, PEGDA has been widely utilized in numerous biomedical and oral delivery applications because of its cytocompatibility, non-toxicity, and simplicity in handling [57–59]. Here PEGDA700 was used as a crosslinking agent, participating in the polymerization and in the solidification of the buccal films. Its ability to form a cross-linked network allows for controlled drug release. The molecular weight of 700 gives flexibility, elasticity and strength to the buccal films. In a previous study, we have reported NMR analysis on PEGDA700, and it was concluded that after printing and photopolymerization, all

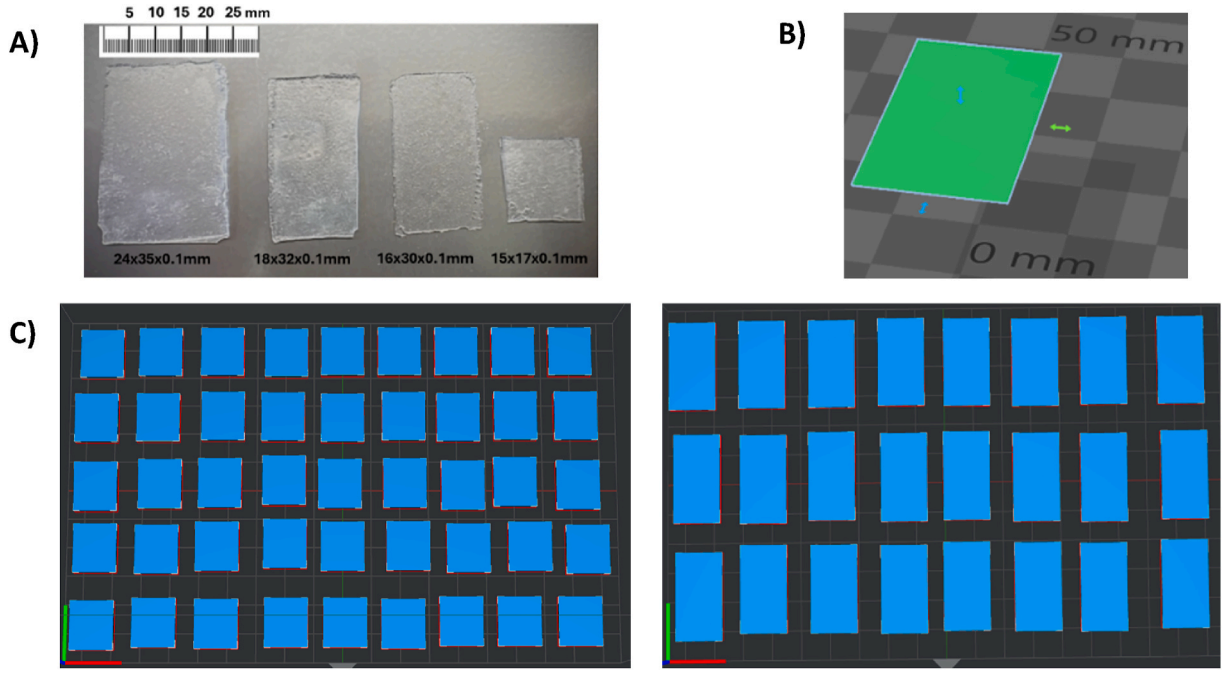

Fig. 2. A) Optical image of the four different sizes of BUP·HCl buccal films, with a scale bar measured in millimeters B) design of the 3D printed buccal films to the AutoCAD software C) scalability of the 15x17 × 0.1 mm and 16x30 × 0.1 mm printed buccal films into two building platforms.

Table 2
Optimized printing parameters for the fabrication of BUP·HCl buccal films.

Parameters	Values
Layer thickness	0.050 mm
Initial exposure	60 s
Exposure time	5.5 s
Rising high	9 mm
Motor speed	5 mm/s
Turn off delay	4 s
Bottom exposure layer	3

monomers that might have toxic effects were eliminated [53]. PEGDA700, is also miscible with water so both can be blended for the development of printable inks. PEG200 is used as a plasticizer to form flexible BUP·HCl buccal films which are less brittle with smooth surface. A major advantage of PEG200 is the disruption of the resin polymerization process, leading to the formation of water soluble fragments within the printed structure. These fragments promote faster dissolution rates of the drug. Polyox 10N, is used to enhance the adhesion of the buccal films to the oral mucosa.

3.2. Films physical characteristics

The physical characteristics of four different buccal films in terms of weight and dimensions are illustrated in Table 3. It can be seen that LCD offers high print accuracy and reproducibility where the dimensions of the printed films are in good agreement with initial designs. To test the linearity of the weight and surface area of the produced films, a graph of these two data sets was plotted. A distinct trend was observed, implying that there was some degree of linearity between the two variables.

Table 3
Dimensions and weights after dehydration of the produced buccal films (n = 10).

Sizes	Length (mm)	Width (mm)	Height (mm)	Weight (mg)
15x17x0.1	15 ± 0.40	17 ± 0.38	0.1 ± 0.02	106.6 ± 2.10
16x30x0.1	16 ± 0.39	30 ± 0.42	0.1 ± 0.02	232.2 ± 2.02
18x32x0.1	18 ± 0.36	32 ± 0.40	0.1 ± 0.03	235.8 ± 3.10
24x35x0.1	24 ± 0.41	35 ± 0.37	0.1 ± 0.01	283.7 ± 2.50

3.3. Physicochemical characterization for 3D printed buccal films

TGA was conducted over a temperature range of 25 °C–350 °C to assess the thermal stability of BUP·HCl. As illustrated in Fig. 3, 96 % of the drug remained stable up to 170 °C. The melting point of BUP·HCl typically falls between 170 °C and 233 °C. However, at 233 °C, BUP·HCl experienced significant thermal degradation, with 95.85 % of the drug to be degraded. Since the printing process occurred at room temperature, no BUP·HCl degradation was detected, based on TGA analysis.

DSC was further used to analyse the physical state of BUP·HCl in the printed buccal films. Fig. 4 shows that bulk BUP·HCl exhibited a melting endotherm at 240 °C, followed by a sharp exothermic peak at 256 °C, indicating the onset of drug degradation. In the 3D printed films the BUP·HCl was found in amorphous state as the melting endotherm disappeared due to the solubilisation in the excipients comprising the ink. For comparison reasons, placebo films were produced; both the placebo and BUP·HCl films exhibit a step change at 117 °C and 136 °C, respectively, which can be attribute to the presence of H_2O in the printing composition.

Additional analysis was performed using XRPD to investigate the drug state in the printed films. As shown in Fig. 5, no diffraction peaks, corresponding to BUP·HCl, were detected in the printed films. These findings support the DSC results, indicating that BUP·HCl is likely molecularly dispersed within the printed structures. The two peaks shown in the placebo and BUP·HCl buccal films are attributed to polyox 10N.

3.4. SEM analysis

SEM imaging was employed to observe the surface microstructure of the fabricated films. Fig. 6 shows the surface (A), and the cross-section (B, C) of the printed structures. The presence of PEG200, disrupt the full polymerization process of PEGDA, this disruption allows the drug to dissolve and be released from the buccal film [52].

The surface morphology of the printed films was also evaluated

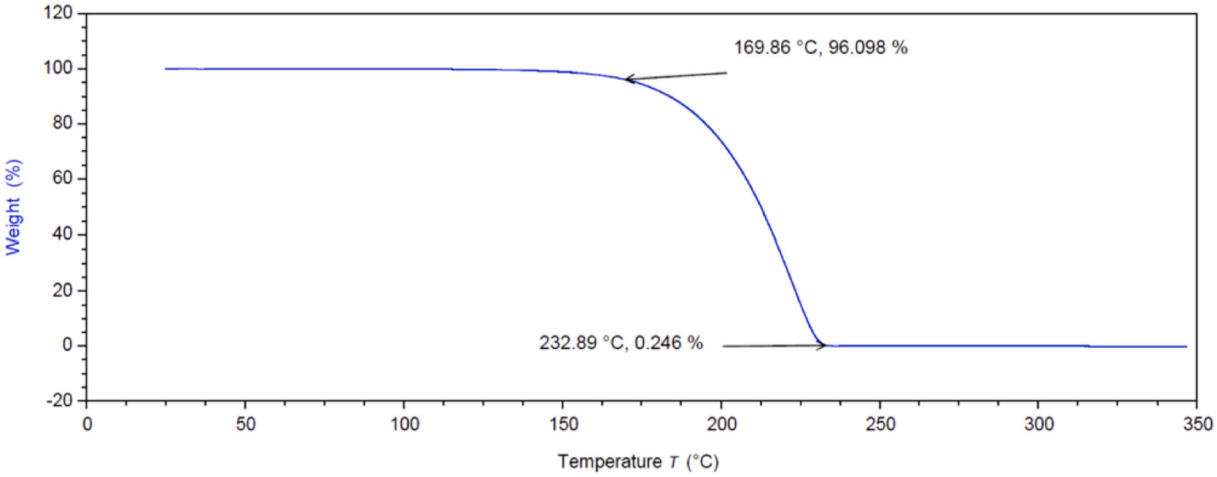

Fig. 3. Thermal gravimetric analysis of BUP·HCl.

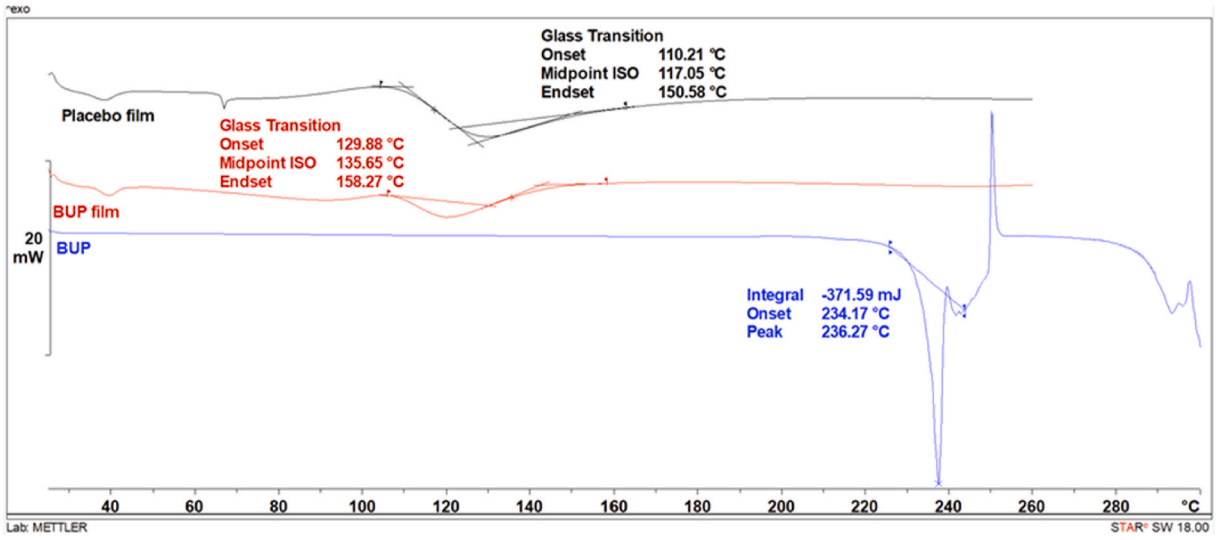

Fig. 4. DSC thermograms of bulk BUP·HCl, placebo and drug loaded films.

before and after swelling, although this data is not included here. The analysis showed that the "as made" films presented a compact surface due to the crosslinking of monomers within the polymer matrix. In contrast, the swollen films exhibited several pores when exposed to the dissolution medium. These results indicate that the presence of PEG200 led to the formation of pores due to the fast polymer hydration. Consequently, faster drug release could be observed due to that as the drug diffuses through the micropore channels in the printed structure.

3.5. *In vitro dissolution studies and mathematical analysis*

For all printed buccal films the drug content was determined using UV–Vis analysis and it was found to vary from 99.6 % to 101.3 %, which aligns with the acceptable percentage range according to USP standards.

In a previous work, for the development of PEGDA700 printed tablets, BUP·HCl presented sustained release over a period of 5 h. However, in the current study, the formation of thin films resulted in immediate release of bulk BUP·HCl due to the high surface and thin dimensions of the printed structures when compared to tablets [52]. As a result, the presence of PEGDA700, which has shown to significantly delay drug release by affecting diffusion (due to crosslinking), did not have any impact on the release of the drug from the buccal films. Another notable finding is that the thin films remained intact and did not dissolve even after 24 h in the media (Fig. 7, inset). This is attributed to the strong covalent bonds created during the crosslinking of the polymerized resin, which prevented the dissolution of the film.

As shown in Fig. 7, all printed films presented immediate BUP·HCl release patterns for about 4–8.5 min. The larger the size of the film, the greater the exposed surface to the dissolution media, and the faster the drug release. In the first minute, it appears that all four films presented the same rate where around 30 % of the drug was released. However, in the following minutes, the effect of the film surface area on the drug release can be easily observed with the rates increasing in an ascending order from the films with the smaller dimensions to the larger ones. Nevertheless, the BUP·HCl release patterns showed complete release in less than 10 min.

3.6. *Ex vivo permeation studies*

The cumulative percentage of BUP·HCl permeated through the porcine buccal mucosa from the 3D-printed buccal film is illustrated in Fig. 8. BUP·HCl was able to cross the mucosa and reach the receptor fluid, with the amount of API increasing over time. After 120 min 52.0 % of BUP·HCl was successfully permeated, showing the ability of the printed films to promote buccal delivery. In addition, the results for steady-state flux (J_S) – 133.98 μg/cm^2/h and lag time (T_L) – 0.35 h

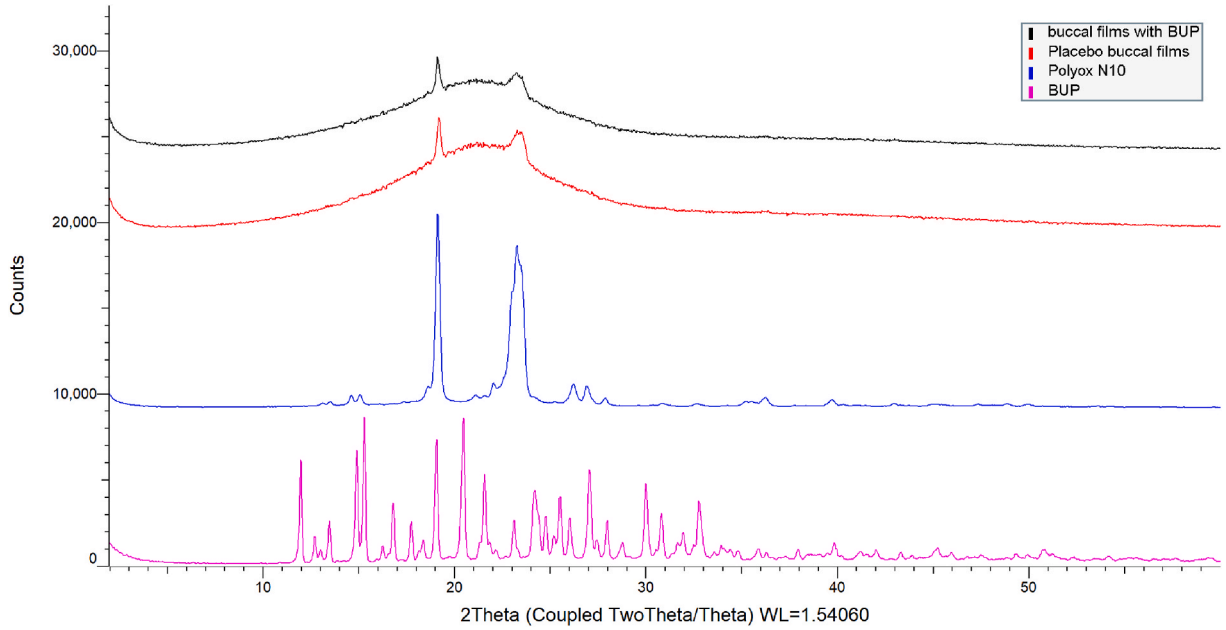

Fig. 5. X-Ray Powder Diffraction of bulk BUP·HCl, placebo and drug loaded films.

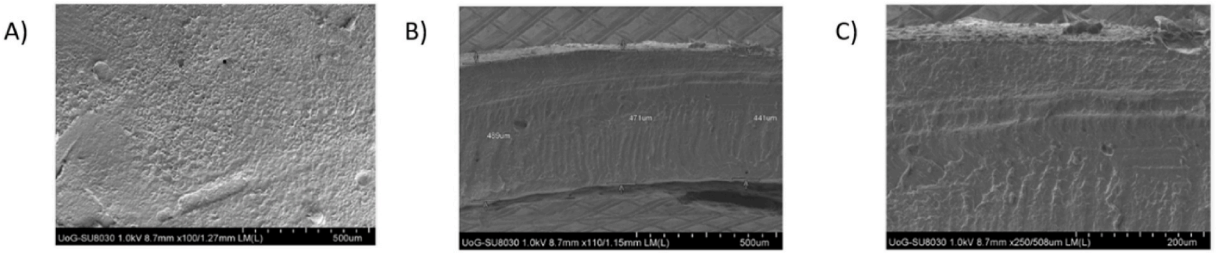

Fig. 6. SEM figures of BUP·HCl 3D printed buccal films: (A) surface view, magnification ×100 (B) Side view of the buccal film, magnification ×110; (C) Closer view of the side view, magnification ×250.

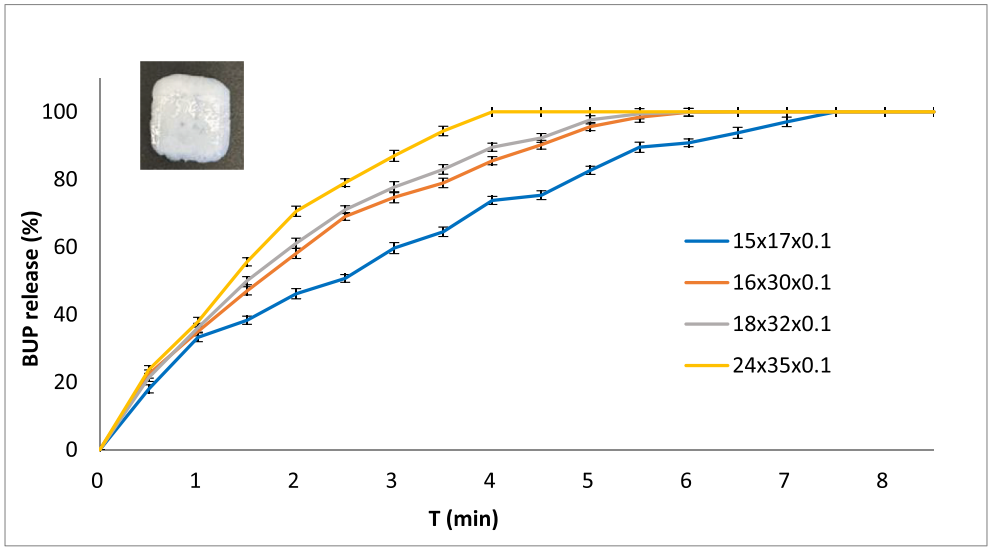

Fig. 7. Dissolution profiles of four different sizes of BUP·HCl 3D printed buccal films. Results represent the mean value (n = 3, SD < 2). Inset: 3D printed buccal films after 24 h of dissolution.

indicate a significant rate at which the drug permeates through the membrane and a rapid onset, supporting the potential of this formulation for buccal delivery. As expected, the amount of drug permeated was significantly lower than the quantity dissolved. This can be explained due to the membrane's barrier properties, which control molecular transport; the time required for permeation, and also the fluid volume in

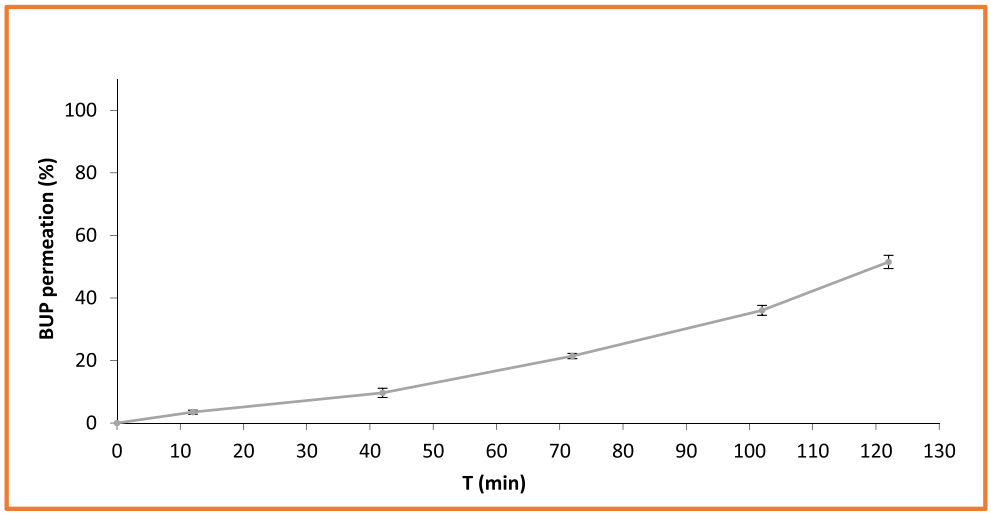

Fig. 8. Cumulative percentage of BUP·HCl permeated from the 3D-printed buccal films. Results were expressed as mean ± SD (n = 2).

the experimental setup. The favourable permeability observed may be attributed to the BUP·HCl features of a small size and logP of 3.21, as it is well-known that small molecules with logP values between 1.6 and 3.3 are rapidly absorbed [60,61]. Moreover, the use of PEG could also have a positive impact on permeability, since it is described in the literature as a permeation enhancer for different types of biological membranes [60,62,63].

Nevertheless, as buccal films are used for prolonged drug deliver the obtained BUP·HCl permeation rates were considered satisfactory [47].

3.7. Water loss rate

The water loss rate was calculated using Equation (1) and is presented in Fig. 9. In the first 2 h, almost 40 % of the water evaporated while for 4–10 h, there was no significant water loss. As the initial ink comprises of 35 % water, the findings indicate complete water evaporation within 4 h.

3.8. Determination of swelling ratio (SR)

As shown Fig. 10, the swelling ratio was observed over a 24-h period. The molecular weight of PEGDA has a major influence on the swelling ratio. It is likely that the higher molecular weight, significantly reduces the availability of free acrylate groups, which are involved in forming covalent crosslinks. As a result, there is a lower degree of crosslinking and an increased elastic behaviour of the PEGDA chains, leading to greater water absorption capacity [64,65]. The molecular weight, chain length, and mobility of the monomers are key factors in photopolymerization, affecting the extent of crosslinking [66]. Longer chains generally have reduced mobility, which decreases further during photopolymerization, limiting the movement of chains towards radical groups [67]. This effect reduces covalent crosslink formation and enlarges the mesh size, promoting increased water uptake. The swelling of the films correlates with the swelling observed in publications where tablets were printed using the VAT polymerization 3D printer family with similar excipients [51,53,68].

3.9. Adhesion and puncture strength studies

Placebo and BUP·HCl buccal films were compared regarding their adhesion and puncture strength properties. Because the films were printed in small rectangular strips, their mechanical strength was measured using probe puncture method rather than the commonly used tensile testing which requires vertically stretching between two grips. Fig. 11 (A & B) shows the adhesive (PAF, TWA and cohesiveness) profiles for the placebo (15x17 × 0.1 mm) and drug loaded films (16x30 ×

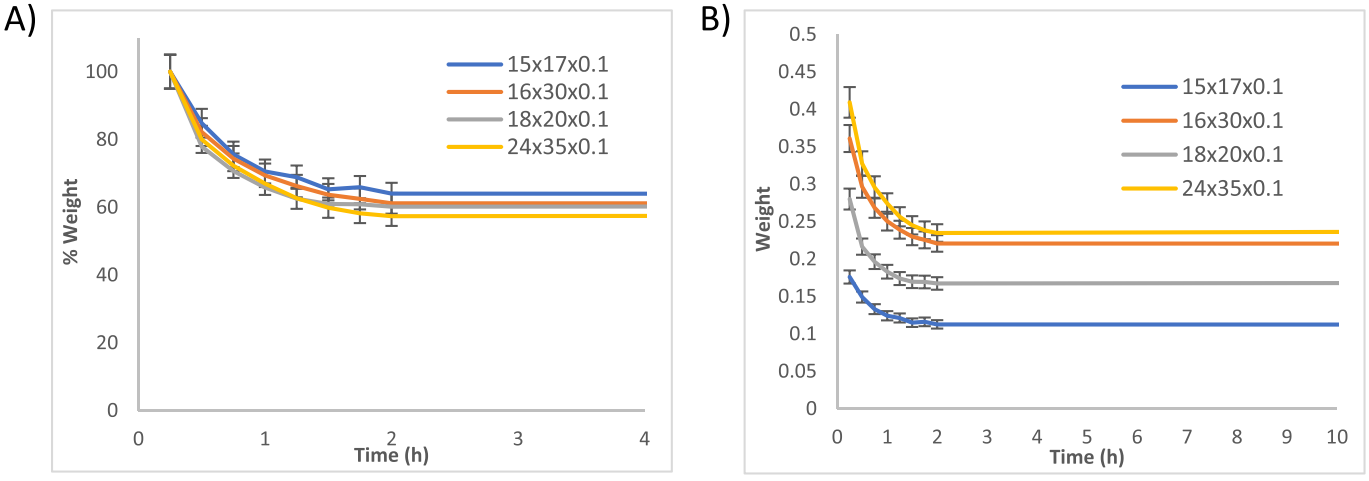

Fig. 9. A) The films relative water weight with the time of the measurement, B) The actual weight loss with the time of the measurement (SD values are <0.001 therefore do not appear in the graph).

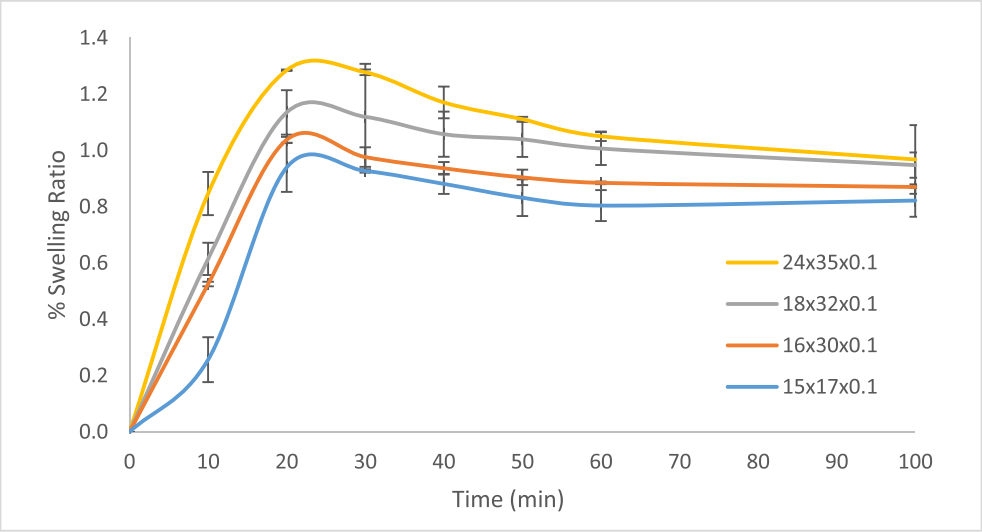

Fig. 10. Swelling ratio of the four different sizes of the buccal films in aqueous media of pH = 6.8.

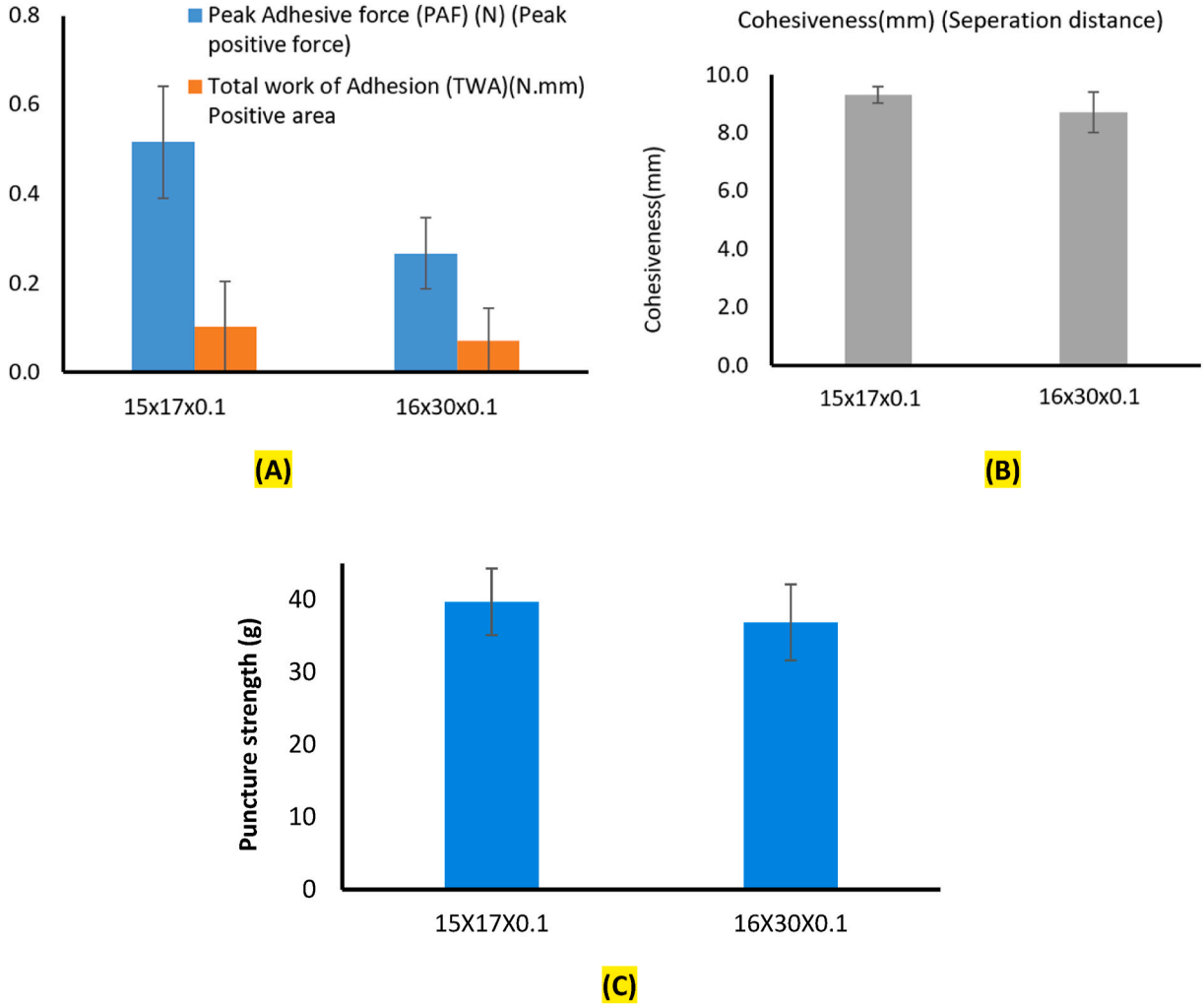

Fig. 11. A) The Peak Adhesive force (PAF) and the Total work of Adhesion (TWA) for the placebo buccal film (15x17 × 0.1 mm) and of the BUP·HCl loaded buccal film (16x30 × 0.1 mm), B) The Cohesiveness (mm) for the placebo buccal film (15x17 × 0.1 mm) and of the BUP·HCl loaded buccal film (16x30 × 0.1 mm). and (C) the puncture strength (g) of the placebo and BUP.HCl loaded films.

0.1 mm). The placebo formulation showed significantly higher PAF than the drug loaded film, however, no marked differences were observed for TWA and cohesiveness. In general, the PAF and TWA values were relatively lower than other polyethylene oxide based films published in the literature [69] which showed PAF values between 0.56 and 0.84N and TWA between 0.37 and 0.52Nmm. This can be attributed to the relatively low amount of adhesive polymer (3 % polyox 10N) compared to the very high amounts of PEG200 which acts as plasticizer for the printed films and can therefore make the formulation slippery, thus lowering the adhesive bond formation. On the other hand, the cohesiveness values were significantly higher than that reported by Pawar et al. [69]. Further, the films prepared by Pawar et al., also contained carrageenan as a modifying polymer and therefore produced more compact and denser films. Therefore, overall, the adhesive profiles are appropriate to allow the films to remain in place for long enough to allow drug release and subsequent permeation. The puncture strength values (Fig. 11C) were similar for both placebo and BUP.HCl films, which suggests that the drug loading did not significantly alter the mechanical behavior of the films.

4. Conclusions

In this study, LCD printing technology was implemented for the development of BUP·HCl buccal thin films. The 3D printed films demonstrate good *ex vivo* adhesion to the oral mucosa due to the presence of polyethylene oxide. The permeation of BUP·HCl through porcine buccal mucosa was satisfactory demonstrating the capacity of printable films to promote buccal delivery. By adjusting the size of printed films it was feasible to develop personalized dosage of various strengths that potentially could meet the needs of individual patients. LCD printing technology holds significant potential for creating personalized dosage forms at the point of care, owing to its rapid printing speeds and high precision. This study tested the flexibility of the films on a texture analyser, however, given its importance for patient compliance, it will be useful to compare the flexibilities of the 3D printed BUP.HCl films with commercially available BUP films.

CRediT authorship contribution statement

Chrystalla Protopapa: Writing – review & editing, Writing – original draft, Software, Investigation, Formal analysis, Data curation. **Angeliki Siamidi:** Writing – review & editing, Writing – original draft, Validation, Software, Investigation, Formal analysis, Data curation. **Laura Andrade Junqueira:** Software, Methodology, Investigation, Formal analysis, Data curation. **Siva Kolibaka:** Software, Investigation, Formal analysis, Data curation. **Hossam Ahmed:** Methodology, Investigation, Formal analysis, Data curation. **Joshua Boateng:** Methodology, Investigation, Formal analysis, Data curation. **Dennis Douroumis:** Writing – review & editing, Writing – original draft, Visualization, Supervision, Software, Resources, Project administration, Methodology, Investigation, Formal analysis, Data curation, Conceptualization. **Marilena Vlachou:** Writing – review & editing, Writing – original draft, Supervision, Resources, Project administration, Funding acquisition, Conceptualization.

Declaration of competing interest

The authors declare that they have no known competing financial interests or personal relationships that could have appeared to influence the work reported in this paper.

Acknowledgments

The research work was supported by the Hellenic Foundation for Research and Innovation (HFRI) under the 5th Call for HFRI PhD Fellowships grant to C.P. (Fellowship Number: 20610).

Data availability

Data will be made available on request.

References

[1] C. Ferrero, L. Urpí, A. Aguilar-de-Leyva, G. Mora-Castaño, V. Linares, M. Millán-Jiménez, et al., Application of ultrasound-assisted compression and 3D-printing semi-solid extrusion techniques to the development of sustained-release drug delivery systems based on a novel biodegradable aliphatic copolyester, J. Drug Deliv. Sci. Technol. 95 (2024) 1–12, https://doi.org/10.1016/j.jddst.2024.105652.
[2] M. Vlachou, A. Siamidi, C. Protopapa, I. Sotiropoulou, A review on the colours, flavours and shapes used in paediatric 3D printed oral solid dosage forms, RPS Pharm Pharmacol Reports 2 (2023) 1–11, https://doi.org/10.1093/rpsppr/rqad009.
[3] NHS England, Improving Outcomes Through Personalised, vols. 1–18, 2016.
[4] P. Khatri, M.K. Shah, N. Vora, Formulation strategies for solid oral dosage form using 3D printing technology: a mini-review, J. Drug Deliv. Sci. Technol. 46 (2018) 148–155, https://doi.org/10.1016/j.jddst.2018.05.009.
[5] D. Douroumis, 3D printing of pharmaceutical and medical applications: a new era, Pharm. Res. 36 (2019), https://doi.org/10.1007/s11095-019-2575-x.
[6] I. Seoane-Viaño, P. Januskaite, C. Alvarez-Lorenzo, A.W. Basit, A. Goyanes, Semi-solid extrusion 3D printing in drug delivery and biomedicine: personalised solutions for healthcare challenges, J. Contr. Release 332 (2021) 367–389, https://doi.org/10.1016/j.jconrel.2021.02.027.
[7] M. Nizam, R. Purohit, M. Taufik, 3D printing in healthcare: a review on drug printing, challenges and future perspectives, Mater. Today Commun. 40 (2024) 110199, https://doi.org/10.1016/j.mtcomm.2024.110199.
[8] C. Protopapa, A. Siamidi, S.S. Kolipaka, L.A. Junqueira, D. Douroumis, M. Vlachou, In vitro profile of hydrocortisone release from three-dimensionally printed paediatric mini-tablets, Pharmaceutics 16 (2024) 385, https://doi.org/10.3390/pharmaceutics16030385.
[9] R. Parhi, A review of three-dimensional printing for pharmaceutical applications: quality control, risk assessment and future perspectives, J. Drug Deliv. Sci. Technol. 64 (2021) 102571, https://doi.org/10.1016/j.jddst.2021.102571.
[10] Marilena Vlachou, Angeliki Siamidi, Chrystalla Protopapa, Extrusion-based 3D printing methods for oral solid dosage forms, in: 3D 4D Print. Methods Pharm. Manuf. Pers. Drug Deliv., Springer, 2023, pp. 195–218.
[11] V.R. Kulkarni, T. Saha, B. Raj Giri, A. Lu, S.C. Das, M. Maniruzzaman, Recent advancements in pharmaceutical 3D printing industry, J. Drug Deliv. Sci. Technol. 100 (2024) 106072, https://doi.org/10.1016/j.jddst.2024.106072.
[12] X. Xu, A. Awad, P. Robles-Martinez, S. Gaisford, A. Goyanes, A.W. Basit, Vat photopolymerization 3D printing for advanced drug delivery and medical device applications, J. Contr. Release 329 (2021) 743–757, https://doi.org/10.1016/j.jconrel.2020.10.008.
[13] A. Raina, M.I.U. Haq, M. Javaid, S. Rab, A. Haleem, 4D printing for automotive industry applications, J Inst Eng Ser D 102 (2021) 521–529, https://doi.org/10.1007/s40033-021-00284-z.
[14] A.T. Chatzitaki, G. Eleftheriadis, K. Tsongas, D. Tzetzis, A. Spyros, I.S. Vizirianakis, et al., Fabrication of 3D-printed octreotide acetate-loaded oral solid dosage forms by means of semi-solid extrusion printing, Int. J. Pharm. 632 (2023) 122569, https://doi.org/10.1016/j.ijpharm.2022.122569.
[15] P. Zgouro, O.L. Katsamenis, T. Moschakis, G.K. Eleftheriadis, A.S. Kyriakidis, K. Chachlioutaki, et al., A floating 3D printed polypill formulation for the coadministration and sustained release of antihypertensive drugs, Int. J. Pharm. 655 (2024) 124058, https://doi.org/10.1016/j.ijpharm.2024.124058.
[16] O.A. Mohamed, S.H. Masood, J.L. Bhowmik, Optimization of fused deposition modeling process parameters: a review of current research and future prospects, Adv. Manuf. 3 (2015) 42–53, https://doi.org/10.1007/s40436-014-0097-7.
[17] A. Jandyal, I. Chaturvedi, I. Wazir, A. Raina, M.I. Ul Haq, 3D printing – a review of processes, materials and applications in industry 4.0, Sustain Oper Comput 3 (2022) 33–42, https://doi.org/10.1016/j.susoc.2021.09.004.
[18] G.K. Eleftheriadis, C. Ritzoulis, N. Bouropoulos, D. Tzetzis, D.A. Andreadis, J. Boetker, et al., Unidirectional drug release from 3D printed mucoadhesive buccal films using FDM technology: in vitro and ex vivo evaluation, Eur. J. Pharm. Biopharm. 144 (2019) 180–192, https://doi.org/10.1016/j.ejpb.2019.09.018.
[19] S. Abdella, F. Afinjuomo, Y. Song, R. Upton, S. Garg, 3D printed bilayer mucoadhesive buccal film of estradiol: impact of design on film properties, release kinetics and predicted in vivo performance, Int. J. Pharm. 628 (2022) 122324, https://doi.org/10.1016/j.ijpharm.2022.122324.
[20] Konstantina Chachlioutaki, Xiunan Li, Savvas Koltsakidis, Hend E. Abdelhakim, Nikolaos Bouropoulos, Dimitrios Tzetzis, Christina Karavasili Dgf, How sugar types and fabrication methods affect palatability in paediatric-friendly oromucosal pullulan films of chlorpromazine hydrochloride, Carbohydr. Polym. (2021) 101890, https://doi.org/10.1016/j.carbpol.2024.122802.
[21] M. Elbadawi, D. Nikjoo, T. Gustafsson, S. Gaisford, A.W. Basit, Pressure-assisted microsyringe 3D printing of oral films based on pullulan and hydroxypropyl methylcellulose, Int. J. Pharm. 595 (2021) 120197, https://doi.org/10.1016/j.ijpharm.2021.120197.
[22] Jovanovic Marija, Petrović Miloš, Cvijic Sandra, Tomic Natasa, Stojanovic Dusica, Ibric Svetlana, et al., 3D printed buccal films for prolonged-release of propranolol hydrochloride: development, characterization and bioavailability prediction, Pharmaceutics 13 (2021).

[23] J.W. Anderson, F.L. Greenway, K. Fujioka, K.M. Gadde, J. McKenney, P.M. O'Neil, Bupropion SR enhances weight loss: a 48-Week double-blind, Placebo- controlled trial, Obes. Res. 10 (2002) 633–641, https://doi.org/10.1038/oby.2002.86.
[24] R. Richmond, N. Zwar, Review of bupropion for smoking cessation, Drug Alcohol Rev. 22 (2003) 203–220, https://doi.org/10.1080/09595230100100642.
[25] K.F. Foley, K.P. DeSanty, R.E. Kast, Bupropion: pharmacology and therapeutic applications, Expert Rev. Neurother. 6 (2006) 1249–1265, https://doi.org/10.1586/14737175.6.9.1249.
[26] Linda P. Dwoskin, Anthony S. Rauhut, Kelley A. King-Pospisil, MTB. Review of the Pharmacology, Clinical profile of bupropion, an antidepressant and tobacco use cessation agent, CNS Drug Rev. 12 (2006) 178–207.
[27] J.W. Jefferson, J.F. Pradko, K.T. Muir, Bupropion for major depressive disorder: pharmacokinetic and formulation considerations, Clin. Ther. 27 (2005) 1685–1695, https://doi.org/10.1016/j.clinthera.2005.11.011.
[28] A.J. Alberg, M.J. Carpenter, Enhancing the effectiveness of smoking cessation interventions: a cancer prevention imperative, J. Natl. Cancer Inst. 104 (2012) 260–262, https://doi.org/10.1093/jnci/djr558.
[29] K. Patel, S. Allen, M.N. Haque, I. Angelescu, D. Baumeister, D.K. Tracy, Bupropion: a systematic review and meta-analysis of effectiveness as an antidepressant, Ther Adv Psychopharmacol 6 (2015) 99–144, https://doi.org/10.1177/2045125316629071.
[30] Moser P. Bupropion, A review of its use in the management of major depressive disorder, XPharm Compr Pharmacol Ref 68 (2008) 1–4, https://doi.org/10.1016/B978-008055232-3.64054-1.
[31] D.S. Baldwin, G.I. Papakostas, Symptoms of fatigue and sleepiness in major depressive disorder, J. Clin. Psychiatry 67 (2006) 9–15.
[32] M. Fava, A.J. Rush, M.E. Thase, A. Clayton, S.M. Stahl, J.F. Pradko, et al., 15 years of clinical experience with bupropion HCl: from bupropion to bupropion SR to bupropion XL, Prim. Care Companion J. Clin. Psychiatry 7 (2005) 106–113, https://doi.org/10.4088/pcc.v07n0305.
[33] Pharmacists AA of P, What is bupropion and what does it treat? Natl Alliance Ment Illn 69–93 (2022), https://doi.org/10.1017/9781009053396.007.
[34] MR Huecker, A Smiley, Saadabadi A. Bupropion, In: StatPearls [Internet]. Treasure Island (FL) [Updated 2024 Sep 2], StatPearls Publishing, 2025. Available from: https://www.ncbi.nlm.nih.gov/books/NBK470212/.
[35] D.J. McCabe, E. McGillis, B.A. Willenbring, Clinical effects of intravenous bupropion misuse reported to a regional poison center, Am. J. Emerg. Med. 47 (2021) 86–89, https://doi.org/10.1016/j.ajem.2021.03.061.
[36] M.I. Damaj, S.D. Grabus, H.A. Navarro, R.E. Vann, J.A. Warner, L.S. King, et al., Effects of hydroxymetabolites of bupropion on nicotine dependence behavior in mice, J. Pharmacol. Exp. Therapeut. 334 (2010) 1087–1095, https://doi.org/10.1124/jpet.110.166850.
[37] J. Davidson, Seizures and bupropion: a review, J. Clin. Psychiatry 50 (1989) 256–261.
[38] S.A. Al-Abri, J.P. Orengo, S. Hayashi, K.L. Thoren, N.L. Benowitz, K.R. Olson, Delayed bupropion cardiotoxicity associated with elevated serum concentrations of bupropion but not hydroxybupropion, Clin. Toxicol. 51 (2013) 1230–1234, https://doi.org/10.3109/15563650.2013.849349.
[39] S. Pushpakom, F. Iorio, P.A. Eyers, K.J. Escott, S. Hopper, A. Wells, et al., Drug repurposing: progress, challenges and recommendations, Nat. Rev. Drug Discov. 18 (2018) 41–58, https://doi.org/10.1038/nrd.2018.168.
[40] P. Rana, R.S.R. Murthy, Formulation and evaluation of mucoadhesive buccal films impregnated with carvedilol nanosuspension: a potential approach for delivery of drugs having high first-pass metabolism, Drug Deliv. 20 (2013) 224–235, https://doi.org/10.3109/10717544.2013.779331.
[41] S. Jacob, A.B. Nair, S.H.S. Boddu, B. Gorain, N. Sreeharsha, J. Shah, An updated overview of the emerging role of patch and film-based buccal delivery systems, Pharmaceutics 13 (2021), https://doi.org/10.3390/pharmaceutics13081206.
[42] M.S. Alqahtani, M. Kazi, M.A. Alsenaidy, M.Z. Ahmad, Advances in oral drug delivery, Front. Pharmacol. 12 (2021), https://doi.org/10.3389/fphar.2021.618411.
[43] I. Speer, M. Preis, J. Breitkreutz, Dissolution testing of oral film preparations: experimental comparison of compendial and non-compendial methods, Int. J. Pharm. 561 (2019) 124–134, https://doi.org/10.1016/j.ijpharm.2019.02.042.
[44] J.G. Meher, M. Tarai, N.P. Yadav, A. Patnaik, P. Mishra, K.S. Yadav, Development and characterization of cellulose-polymethacrylate mucoadhesive film for buccal delivery of carvedilol, Carbohydr. Polym. 96 (2013) 172–180, https://doi.org/10.1016/j.carbpol.2013.03.076.
[45] F.K. Alanazi, A.A.A. Rahman, G.M. Mahrous, I.A. Alsarra, Formulation and physicochemical characterisation of buccoadhesive films containing ketorolac, J. Drug Deliv. Sci. Technol. 17 (2007) 183–192, https://doi.org/10.1016/S1773-2247(07)50034-1.
[46] L. Shipp, F. Liu, L. Kerai-Varsani, T.C. Okwuosa, Buccal films: a review of therapeutic opportunities, formulations & relevant evaluation approaches, J. Contr. Release 352 (2022) 1071–1092, https://doi.org/10.1016/j.jconrel.2022.10.058.
[47] W. Zhang, C. Xiao, Y. Xiao, B. Tian, D. Gao, W. Fan, et al., An overview of in vitro dissolution testing for film dosage forms, J. Drug Deliv. Sci. Technol. 71 (2022) 103297, https://doi.org/10.1016/j.jddst.2022.103297.
[48] A. Adrover, A. Pedacchia, S. Petralito, R. Spera, In vitro dissolution testing of oral thin films: a comparison between USP 1, USP 2 apparatuses and a new millifluidic flow-through device, Chem. Eng. Res. Des. 95 (2015) 173–178, https://doi.org/10.1016/j.cherd.2014.10.020.
[49] A. Apostolidi, C. Protopapa, A. Siamidi, M. Vlachou, Y. Dotsikas, Dissolution assay of bupropion/naltrexone hydrochloride salts of bilayer composition tablets following the development and validation of a novel HPLC method, Materials 15 (2022), https://doi.org/10.3390/ma15238451.
[50] A.G. Tabriz, D.H.G. Fullbrook, L. Vilain, Y. Derrar, U. Nandi, C. Grau, et al., Personalised tasted masked chewable 3d printed fruit-chews for paediatric patients, Pharmaceutics 13 (2021), https://doi.org/10.3390/pharmaceutics13081301.
[51] P. Robles-Martinez, X. Xu, S.J. Trenfield, A. Awad, A. Goyanes, R. Telford, et al., 3D printing of a multi-layered polypill containing six drugs using a novel stereolithographic method, Pharmaceutics 11 (2019), https://doi.org/10.3390/pharmaceutics11060274.
[52] C. Protopapa, A. Siamidi, L.A. Junqueira, S. Kolipaka, A.G. Tabriz, D. Douroumis, et al., Sustained release of 3D printed bupropion hydrochloride tablets bearing braille imprints for the visually impaired, Int. J. Pharm. 663 (2024) 124594, https://doi.org/10.1016/j.ijpharm.2024.124594.
[53] C. Protopapa, A. Siamidi, A. Sakellaropoulou, S. Kolipaka, L.A. Junqueira, A. G. Tabriz, et al., 3D-Printed melatonin tablets with braille motifs for the visually impaired, Pharmaceuticals 17 (2024) 1–14, https://doi.org/10.3390/ph17081017.
[54] J. Wang, A. Goyanes, S. Gaisford, A.W. Basit, Stereolithographic (SLA) 3D printing of oral modified-release dosage forms, Int. J. Pharm. 503 (2016) 207–212, https://doi.org/10.1016/j.ijpharm.2016.03.016.
[55] P.R. Martinez, A. Goyanes, A.W. Basit, S. Gaisford, Influence of geometry on the drug release profiles of stereolithographic (SLA) 3D-Printed tablets, AAPS PharmSciTech 19 (2018) 3355–3361, https://doi.org/10.1208/s12249-018-1075-3.
[56] N.M.G. Almeida, R. Lima, T.F.R. Alves, M.A. De Rebelo, P. Severino, M.V. Chaud, A novel dosage form for buccal administration of bupropion, Brazilian J Pharm Sci 51 (2015) 91–100, https://doi.org/10.1590/S1984-82502015000100010.
[57] J.P. Mazzoccoli, D.L. Feke, H. Baskaran, P.N. Pintauro, Mechanical and cell viability properties of crosslinked low and high MW PEGDA blends, J. Biomed. Mater. Res. 93 (2010) 558–566, https://doi.org/10.1002/jbm.a.32563. Mechanical.
[58] G.M. Cruise, D.S. Scharp, J.A. Hubbell, Characterization of permeability and network structure of interfacially photopolymerized poly(ethylene glycol) diacrylate hydrogels, Biomaterials 19 (1998) 1287–1294, https://doi.org/10.1016/S0142-9612(98)00025-8.
[59] M.S. Hahn, J.S. Miller, J.L. West, Three-dimensional biochemical and biomechanical patterning of hydrogels for guiding cell behavior, Adv. Mater. 18 (2006) 2679–2684, https://doi.org/10.1002/adma.200600647.
[60] V.V. Nair, P. Cabrera, C. Ramírez-Lecaros, M.O. Jara, D.J. Brayden, J.O. Morales, Buccal delivery of small molecules and biologics: of mucoadhesive polymers, films, and nanoparticles – an update, Int. J. Pharm. 636 (2023) 122789, https://doi.org/10.1016/j.ijpharm.2023.122789.
[61] A.D. Earhart, S. Patrikeeva, X. Wang, D. Reda Abdelrahman, G.D.V. Hankins, M. S. Ahmed, et al., Transplacental transfer and metabolism of bupropion, J Matern Neonatal Med 23 (2010) 409–416, https://doi.org/10.3109/14767050903168424.
[62] J. Lee, I.W. Kellaway, Combined effect of oleic acid and polyethylene glycol 200 on buccal permeation of [D-Ala2, D-Leu5]enkephalin from a cubic phase of glyceryl monooleate, Int. J. Pharm. 204 (2000) 137–144, https://doi.org/10.1016/S0378-5173(00)00490-7.
[63] H.T. Isa, C.K. Enggi, S. Sulistiawati, K. Agus, S. Wijaya, A.D. Permana, Polyethylene glycol as new permeation enhancer in thermosensitive mucoadhesive hydrogels containing hydrophobic compound for vaginal delivery: an Ex vivo proof of concept study, Biointerface Res Appl Chem 13 (2023) 1–7, https://doi.org/10.33263/BRIAC134.315.
[64] F. Della Sala, M. Biondi, D. Guarnieri, A. Borzacchiello, L. Ambrosio, L. Mayol, Mechanical behavior of bioactive poly(ethylene glycol) diacrylate matrices for biomedical application, J. Mech. Behav. Biomed. Mater. 110 (2020) 103885, https://doi.org/10.1016/j.jmbbm.2020.103885.
[65] A.H. Karoyo, L.D. Wilson, A review on the design and hydration properties of natural polymer-based hydrogels, Materials 14 (2021) 1–36, https://doi.org/10.3390/ma14051095.
[66] H. Ju, B.D. McCloskey, A.C. Sagle, V.A. Kusuma, B.D. Freeman, Preparation and characterization of crosslinked poly(ethylene glycol) diacrylate hydrogels as fouling-resistant membrane coating materials, J. Membr. Sci. 330 (2009) 180–188, https://doi.org/10.1016/j.memsci.2008.12.054.
[67] E. Peris, M.J. Bañuls, Á. Maquieira, R. Puchades, Photopolymerization as a promising method to sense biorecognition events, TrAC - Trends Anal. Chem. 41 (2012) 86–104, https://doi.org/10.1016/j.trac.2012.09.003.
[68] C. Protopapa, A. Siamidi, L.A. Junqueira, S. Kolipaka, A.G. Tabriz, D. Douroumis, et al., Sustained release of 3D printed bupropion hydrochloride tablets bearing braille imprints for the visually impaired, Int. J. Pharm. 663 (2024) 124594, https://doi.org/10.1016/j.ijpharm.2024.124594.
[69] J.S. Boateng, H.V. Pawar, J. Tetteh, Polyox and carrageenan based composite film dressing containing anti-microbial and anti-inflammatory drugs for effective wound healing, Int. J. Pharm. 441 (2013) 181–191, https://doi.org/10.1016/j.ijpharm.2012.11.045.